Molecular BioSystems

Accepted Manuscript

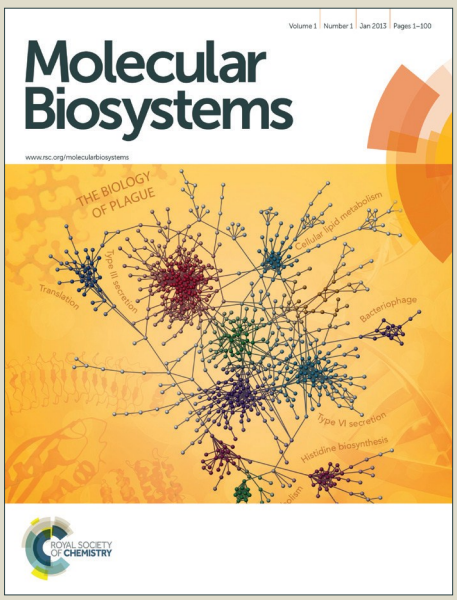

ROYAL SOCIETY OF CHEMISTRY

www.rsc.org/molecularbiosystems

MicroRNAs regulate KDM5 histone demethylases in breast cancer cells

Hélène Denis[1], Olivier Van Grembergen[1], Benjamin Delatte[1], Sarah Dedeurwaerder[1], Pascale Putmans[1], Emilie Calonne[1], Françoise Rothé[2], Christos Sotiriou[2], François Fuks[1] and Rachel Deplus[1,*]

[1]Laboratory of Cancer Epigenetics, Faculty of Medicine, Université Libre de Bruxelles, Brussels, Belgium; [2]Breast Cancer Translational Research Laboratory, Jules Bordet Institute, Université Libre de Bruxelles, Brussels, Belgium

* Corresponding author.

Email: rdeplus@ulb.ac.be

Abstract

MicroRNAs (miRNAs) are small non-coding RNAs that post-transcriptionally regulate gene expression. Alteration of miRNA levels is common in tumors and contributes to the pathogenesis of human malignancies. In the present study we examined the role played by miR-137 in breast tumorigenesis.

We found miR-137 levels to be lower in breast cancer cells than in their non-tumorigenic counterparts and observed reduced proliferation and migration of breast cancer cells overexpressing miR-137. We further identified KDM5B, a histone demethylase known to be involved in breast cancer tumorigenesis, as a target of miR-137. As the involvement of histone demethylases in cancer is still poorly understood and as the role of miRNAs in controlling epigenetic mechanisms in cancer is emerging, we broadened our study to the whole KDM5 histone demethylase family to see if the genes coding for these epigenetic enzymes might be regulated by miRNAs in cancer cells. We discovered that KDM5C is overexpressed in breast cancer cells, providing evidence that miR-138 regulates its expression. We found miR-138 overexpression to affect breast cancer cell proliferation.

Altogether, our findings suggest that miRNAs may regulate KDM5 histone demethylase levels in breast cancer and thereby control breast cancer cell proliferation and migration.

Introduction

Epigenetic mechanisms include DNA methylation, post-translational histone modifications, and chromatin remodelling. They are involved in modulating the structure of chromatin to make it suitable for gene transcription or silencing.[1] An altered epigenomic pattern is a major feature of cancer, and it is now clear that misregulation of histone modifications contributes to human cancer.[2] Histone modification patterns are dynamically regulated by enzymes that add, remove, or read covalent modifications. For instance, histone lysine methyltransferases (KMTs) add methyl groups onto lysine residues of histones, while histone lysine demethylases (KDMs) remove these methyl groups. The contribution of KMTs to cancer has been extensively investigated.[3–6] Although less studied, KDM misregulation appears also to be involved in cancer progression.[3,7] For instance, KDM1A (also known as LSD1) is highly expressed in poorly differentiated neuroblastoma, and pharmacological inhibition of LSD1 reduces neuroblastoma xenograft growth.[8,9] Among the KDMs, we focus here on the KDM5 family and on the possible role of its members in cancer. The KDM5 proteins contain a JmjC domain and are the only KDMs capable of removing from lysine 4 of histone H3 the tri- and di-methyl marks for transcriptionally active chromatin.[10] This enzyme family comprises four members: KDM5A (also known as JARID1A or RBP2); KDM5B (also known as JARID1B or PLU-1); KDM5C, located on the X chromosome (also known as JARID1C or SMCX), and KDM5D, located on the Y chromosome (also known as JARID1D or SMCY).[10] Studies on human malignancies have pointed to a role of two members of the KDM5 family, KDM5A and KDM5B, in cancer development. KDM5A is reported to be translocated in leukemia[11,12] and overexpressed in gastric cancer[13], and its loss has been shown to inhibit tumorigenesis in a mouse cancer model.[14] KDM5B is overexpressed in various types of malignancies[15–18], and its down-regulation suppresses breast cancer growth in a syngenic mouse cancer model.[19] The involvement of KDM5C and KDM5D in carcinogenesis is still less clear.

The fairly recent discovery of the crucial role played by miRNAs has broadened our view of the gene expression - epigenetic regulation network. These approximately 22-nucleotides-long noncoding RNAs negatively regulate the expression of genes, usually through direct imperfect

alignment with the 3' untranslated region (3'UTR) of target mRNAs. This binding causes mRNA translational repression, deadenylation, or degradation.[20,21] More than 1000 different miRNAs have been described in the human genome, and efforts to delineate their specific gene targets are still in progress. MicroRNAs influence multiple biological processes. Importantly, a growing number of reports indicate that they affect cell transformation and tumor progression, including the lethal metastatic phase of cancer.[22–25] Global expression of miRNAs is deregulated in most cancer types, being widely downregulated in tumors as compared to normal tissues.[26] MicroRNAs are crucial regulators of tumorigenesis, where they can function as tumor suppressors or oncogenic miRNAs depending on the targets they regulate.[27,28] For instance, miR-137 expression is decreased in oral squamous cell carcinoma[29] and colorectal cancer[30,31], and its overexpression in the corresponding cancer cells inhibits cell growth, suggesting tumor-suppressive activity.[29,30] Both the biological role of miR-137 and its specific downstream mRNA targets in breast carcinogenesis remain unknown.

Breast cancer is a heterogeneous disease, and with around 500,000 deaths yearly, it is the most frequent cause of cancer death in women.[32,33] Advances in prevention, diagnosis, and treatment are responsible for an increased survival rate[34], but the molecular pathogenesis of breast cancer is not yet fully understood. In the present paper we show that miR-137 levels are lower in breast cancer cells than in their non-tumorigenic counterparts and that miR-137 overexpression in breast cancer cells causes inhibition of growth and migration. We identify the histone demethylase KDM5B as a target of miR-137 and show that KDM5C is also overexpressed in breast cancer cells. We provide evidence that miR-138 negatively regulates the expression of KDM5C and that miR-138 overexpression inhibits breast cancer cell proliferation. Altogether, our results suggest that miR-137 and miR-138 may act as tumor supressor miRNAs in breast cancer.

Results and Discussion

miR-137 is silenced in human breast cancer cell lines

Global miRNA expression is deregulated in most cancer types, being widely downregulated in tumors as compared to normal tissues.[26] In particular, miR-137 expression is decreased in oral squamous cell carcinoma[29] and colorectal cancer[30,31], where miR-137 seems to affect tumor cell growth. To see if miR-137 expression is also reduced in breast cancer, we used TaqMan real-time PCR to measure miR-137 expression in breast cancer cell lines (MCF7, MDA-MB-231, MDA-MB-361, BT20, SKBR3, and ZR-75-1) and in non-tumorigenic human mammary epithelial cell line MCF10A. In all breast cancer cell lines tested, miR-137 expression was found to be lower than in non-tumorigenic cells (Fig. 1A). RNU6B was used control to normalize the expression of target microRNAs, with the copy number being shown at the bottom part of the Figure 1A. Comparaison with a second normal cell line, MCF12A, was performed and the expression of miR-137 was higher in MCF12A as compared to breast cancer cell lines (Fig. S1). We also examined publicly accessible data from ENCODE, which showed the higher expression of miR-137 in normal HMEpC as compared to MCF7 (Fig. S2).

Epigenetic mechanisms such as promoter methylation or histone acetylation can modulate microRNA expression, and aberrant regulation at this level is found in cancer. To investigate whether miR-137 downgulation in breast cancer might result from promoter methylation, we analysed the genomic sequence of the miR-137 gene with the UCSC Genome Browser (http://genome.ucsc.edu). We found that the miR-137 gene is associated with a CpG island (Fig. 1B, upper part). As cancer cells are characterised by hypermethylation of specific CpG island promoters[35], we hypothesised that miR-137 gene might be regulated by DNA methylation in cancer. To examine experimentally the methylation status of the miR-137 promoter, we applied bisulfite pyrosequencing to five CpG sites located respectively 66 bp, 63 bp, 60 bp, 57 bp, and 45 bp upstream of the transcription start site (TSS) of the miR-137 gene. Figure 1B depicts the level of methylation of each CpG site in non-tumorigenic MCF10A and MCF12A cells and in the MCF7, MDA-MB-361, BT20, and ZR-75-1 breast cancer cell lines. For a given cell type, all five CpG sites analyzed tended to show a similar degree of methylation

(Fig. 1B). The miR-137 promoter appeared weakly methylated in non-tumorigenic breast cells (MCF10A and MCF12A) but more highly methylated in all breast cancer cell lines (Fig. 1B). Previous reports showed that miR-137 undergoes promoter methylation in oral squamous cell carcinoma[29], gastric cancer cell lines[36,37], colorectal cancer[30,31] and lung cancer[38] suggesting that miR-137 promoter methylation could be a common and general feature of tumor cells. Previous studies have shown treatment with the demethylating agent 5-aza-2-deoxycytidine (5-aza) to restore miR-137 expression in oral squamous carcinoma cells and some colorectal cancer cells[29,30]. Here, we show that this agent induced significant miR-137 reexpression in breast cancer cells (Fig. S3). It thus appears that miR-137 is silenced in breast tumor cells, but that promoter methylation alone cannot explain the lower levels of miR-137 expression observed. Given the know interplay between DNA methylation and histone deacetylation, we tested if a synergism between these two repressive machineries might explain silencing of miR-137 in breast cancer cells. For this, MCF7 cells were treated with 5-aza and/or TSA. As presented in Figure S3, histone deacetylase inhibitor or DNA methyltransferase inhibitor led to substantial reactivation of miR-137 expression in MCF7 cells. However, combination of 5-aza and TSA didn't show elevated miR-137 expression, suggesting independent regulation by histone deacetylation and DNA methylation of miR-137 expression.

miR-137 overexpression inhibits breast cancer cell proliferation and migration

Having shown that miR-137 is silenced in breast cancer cells, we next performed proliferation assays to determine the functional effects of miR-137 overexpression in these cells. Cell proliferation was evaluated in the xCELLigence system. This instument monitors cellular events in real time without exogenous labeling, through impedance-based technology.[39] It provides a kinetic cell-response profile throughout the experiment, detailing the onset and rate of proliferation. After transfection of MCF7 cells with miR-137 precursors, cell growth was measured every 30 min for 3 days (see Materials and Methods for details). TaqMan real-time PCR analysis (Fig. S4) confirmed the overexpression of mature miR-137 in the transfected cells. As compared to control cells (ctrl pre-miR), pre-miR-137-transfected cells showed strongly reduced proliferation (Fig. 2A). Figure 2B, where the rate of cell

proliferation is estimated as the mean slope of the cell growth curves for three independent experiments, shows that this rate was reduced by more than 70% in the pre-miR-137-transfected breast cancer cells.

We then evaluated the effect of miR-137 on the migration behavior of breast cancer cells. Cell migration kinetics was recorded in real time with the xCELLigence system (see scheme of the system used in Fig. S5). As is common[40], we performed the migration assays with MDA-MB-231 cells, using fetal bovine serum (FBS) as a chemoattractant. The cells were transfected with miRNA precursors and overexpression of the mature miR-137 was confirmed (Fig. S6). Cell migration was then measured every 30 min for 24h (Fig. 2C). Without any chemoattractant in the medium of the lower chamber, the cells did not migrate (ctrl pre-miR and pre-miR-137, grey and yellow curves respectively in Fig. 2C). When FBS was used as a chemotaxis inducer, the cells migrated to the lower chamber. We found the control cells (ctrl pre-miR, black curve in Fig. 2C) to migrate faster than the pre-miR-137-transfected cells (pre-miR-137, red curve in Fig. 2C). We focused on the first 4 hours of the migration kinetics (cf Material and Methods) to calculate the rate of cell migration, represented in Fig. 2D as the mean slope of the cell migration curves from three independent experiments. Cell migration was found to decrease by 40% in response to miR-137 overexpression (Fig. 2D). Our findings thus suggest that miR-137 reduces both the proliferation and migration of breast cancer cells.

KDM5B is a direct target of miR-137

Although miRNAs appear to regulate the expression of many different genes, their function in tumorigenesis might be due to regulation of a few specific ones.[41] To determine the potential target of miR-137 in breast cancer, we looked at the different gene targets described in the literature.[42–45] Of particular interest was a study on mouse ES cells, where miR-137 was shown to repress the histone demethylase KDM5B (also known as PLU-1 or JARID1B) and to be required for proper ES cell differentiation.[44] Interestingly, KDM5B is frequently overexpressed in breast cancer, and KDM5B knockdown impairs the proliferative capacity of MCF7 breast cancer cells.[15,17,19] On the basis of these studies, we hypothesized that miR-137 might affect the proliferation of breast cancer cells by targeting

KDM5B. To test this hypothesis, we first performed western blotting using an anti-KDM5B in breast cancer cells (BT20, MCF7, MDA-MB-231, MDA-MB-361, SKBR3, and ZR-75-1) and non-tumorigenic cells (MCF10A). As shown in Figure 3A, breast cancer cell lines harbored higher levels of KDM5B compared to non-tumorigenic mammary cells, sugesting a potential link between miR-137 expression and decreased KDM5B protein level. To confirm that miR-137 regulates KDM5B in breast cancer cells, we transiently transfected MCF7 cells with pre-miR-137 and evaluated the KDM5B mRNA and protein levels. We used MCF7 cells for this experiment because they have a high level of endogenous KDM5B expression (Fig. 3A)[15,17] and undetected levels of miR-137 (Fig. 1A). The KDM5B transcript level (assessed by RT-qPCR) was found to significantly reduced (by ~30%) in pre-miR-137-transfected MCF7 cells (Fig. 3B). Similar results were also obtained in two other cancer cell lines, MDA-MB-231 and MDA-MD-361 (Fig. S7), suggesting a common feature in breast cancer cells. The fact that this transcript-level effect is moderate is not surprising : miR-137 might predominantly affect the translational efficiency, as shown in the literature for other miRNAs.[46] Immunoblot analyses with an antibody targeting KDM5B revealed significantly reduced levels of this protein in miR-137-expressing cancer cells (Fig. 3C). To see if miR-137 regulates KDM5B directly, we cloned into a luciferase reporter vector 25 bp of the KDM5B 3'UTR, corresponding to the miR-137 target sequence in this UTR (Fig. 3D, upper part). Overexpression of pre-miR-137, but not of control precursors, was found to decrease slightly but reproducibly the activity of the luciferase reporter (Fig. 3D). Taken together, our results show that miR-137 regulates KDM5B in breast cancer cells by directly targeting the KDM5B 3'UTR.

miR-138 regulates the histone demethylase KDM5C in breast cancer

While there are previous reports of KDM5B overexpression in various types of malignancies[15–17], it is not known if other members of the KDM5 histone demethylase family are involved in carcinogenesis generally or in breast tumorigenesis in particular. We therefore found it interesting to assess the role of KDM5C in the context of breast cancer. Immunoblot analysis revealed that KDM5C, like KDM5B (Refs 15, 17 and Fig.3A), is overexpressed in BT20, MCF7, MDA-MB-231, MDA-MB-361, SKBR3, and ZR-75-1 breast cancer cells as compared to non-tumorigenic MCF10A (Fig. 4A). We then

examined whether KDM5C might, like KDM5B (Fig. 3), be regulated by miRNAs in breast tumor cells. We used online prediction tools[47] to identify putative KDM5C-targeting miRNA candidates (data not shown). Individual TaqMan assays showed reduced levels of one candidate miRNA, miR-138, in all the cancer cell lines tested except MDA-MB-231, where it was highly overexpressed (Fig. 4B and Fig. S8). We also examined publicly available data from ENCODE, which showed higher expression of miR-138 in HMEpC versus MCF7 (Fig. S9).

Interestingly, MDA-MB-231 was the cancer cell line where the level of KDM5C protein was lowest (Fig. 4A). Nevertheless, despite a stronger expression of miR-138, KDM5C protein is higher in MDA-MB-231 than in non tumorigenic cells, suggesting an additional mechanism of regulation. This supplemental mechanism need to be identified and could regulated KDM5C transcription through transcription factor or epigenetic regulation, or could also influence translation or protein stability.

We then transiently transfected MCF7 cells, characterized by high levels of endogenous KDM5C and an undetectable level of miR-138 (Figs. 4A and 4B), with pre-miR-138. The cells transfected with pre-miR-138 showed respectively ~20% lower levels of KDM5C transcripts than cells transfected with a control pre-miR (Fig. 4C), and they also showed a substantially decreased KDM5C protein level on western blots (Fig. 4D). In order to examine whether miR-138 could regulate KDM5C directly, the miR-138 target sequence of the KDM5C 3'UTR was cloned into a luciferase reporter vector (Fig. 4E, upper part). Significant decrease of activity of the luciferase reporter was detected after overexpression of pre-miR-138. This was not the case for the control precursors (Fig. 3D). Thus, miR-138 regulates KDM5C in breast cancer cells by directly targeting the KDM5B 3'UTR. Taken together, our data indicate that miR-138 causes downregulation of endogenous KDM5C in human breast tumor cells.

High expression of miR-138 decreases breast cancer cell proliferation

We then examined whether enhanced expression of miR-138 might affect breast cancer cell proliferation. We transfected MCF7 breast cancer cells with pre-miR-138 and monitored cell growth in real time in the xCELLigence system (Fig. 5A). Overexpression of mature miR-138 was confirmed by real-time PCR analysis (Fig. S10). In this experiment, cells transfected with pre-miR-138 showed substantially slower proliferation than control cells (ctrl pre-miR) (Fig. 5A). Figure 5B shows that the proliferation rate, estimated here as the mean slope of the cell growth curves from three independent experiments, was halved when miR-138 was overexpressed. Taken together, our findings show that miR-138 can regulate KDM5C expression in breast cancer cells, and that this miR can affect their proliferation.

Conclusion

In recent years, several reports have highlighted deregulation of miRNA expression in human cancers, including breast cancer.[26,48] For example, downregulation of miR-137 has been observed in oral squamous cell carcinoma and in colorectal cancer.[30,31] We find that miR-137 is also downregulated in breast cancer cells, and this suggests that miR-137 might be a central event in tumorigenesis. Our bisulfite pyrosequencing data show that CpG sites located in the miR-137 promoter are weakly methylated in non-tumorigenic breast cells (MCF10A), but more strongly methylated in breast cancer cell lines. Yet treatment with a DNA methyltransferase inhibitor alone or in combination with histone deacetylase inhibitors did not fully restore miR-137 expression. This indicates that other mechanisms must regulate the miR-137 level. These mechanisms deserve further investigation.

We also provide evidence that miR-137 might play a role in breast tumorigenesis: overexpression of miR-137 in breast cancer cells reduces significantly both the proliferation and the migration of these cells. Identifying miR-137-specific targets is crucial to understanding its possible role in tumorigenesis. Interestingly, we have identified KDM5B, a key histone demethylase involved in breast cancer tumorigenesis[17,19], as a novel miR-137 target. Altogether, both our data and other

published results concerning miR-137 in oral squamous cell carcinoma[29] and colorectal cancer[30,31] suggest that this microRNA may function as a tumor suppressor gene and thus be a good candidate for use in anticancer therapy.

The contribution of histone lysine methyltransferases to cancer has been extensively explored.[3–5] Although less studied, overexpression of histone demethylases has also been implicated in cancer progression.[3] One piece of evidence suggesting that KDM5 H3K4me3 demethylases might participate in tumorigenesis is the observation that KDM5B is overexpressed in several cancers, including breast cancer[15–17,19]. Here we show for the first time that the histone demethylase KDM5C is also overexpressed in breast tumor cells. Additional studies will also be necessary to determine what functional role KDM5C might play in breast carcinogenesis *in vivo*. The relevance of KDM5C to tumor formation and/or metastasis must be investigated in detail.

KDM5 family members might present functional overlap and KDM5 protein might exert their function together. Nevertheless, different tissues tropism[49] or divergent phenotypes of knockout mice[50,51] point also to independent mode of actions. Common and divergent functional properties shared or not by KDM5B and KDM5C and involved in tumorgenesis should be investigated in future.

Over the past few years, miRNAs have been emerging as agents controlling epigenetics in cancer. The importance of this control is underscored by the finding that a number of crucial epigenetic regulators, including key enzymes regulating DNA methylation (DNMT3A and DNMT3B)[52,53], histone methylation (EZH2)[54], and histone deacetylation (HDAC1)[55], are targeted by miRNAs in human cancers. Until our present study, nothing was known regarding the regulation of histone demethylases by miRNAs in carcinogenesis. We demonstrate for the first time that miRNAs can also control KDMs in cancer cells: miR-137 controls the histone demethylase KDM5B, and overexpression of miR-138 affects KDM5C expression in breast cancer cells. We also show that miR-138 overexpression, like miR-137, affects breast cancer cell proliferation. We thus add two new examples illustrating how miRNAs can regulate epigenetic enzymes, here KDMs, in cancer cells.

Altogether, our findings suggest that reduced miRNA levels may contribute to breast tumorigenesis by allowing KDM5 histone demethylases to accumulate to an abnormally high level and thus favoring unchecked cell proliferation and migration. As cancer cells depend on dysregulation of specific miRNAs for proliferation and survival, miRNAs might be prove useful as therapeutic tools favoring tumor regression.

Materials and Methods

Cell lines

MCF10A cells were grown in a 1:1 mixture of DMEM and F12 medium, supplemented with 10% fetal calf serum. MCF12A cells were grown in a 1:1 mixture of Dulbecco's modified Eagle's medium and Ham's F12 medium supplemented with 20 ng/ml Human epidermal growth factor, 100 ng/ml cholera toxin, 0.01 mg/ml bovine insulin, 500 ng/ml hydrocortisone and 5% horse serum. MCF7, SKBR3, and MDA-MB-231 cells were grown in DMEM supplemented with 10% fetal calf serum. ZR-75-1 and MDA-MB-361 cells were grown in RPMI supplemented with 10% fetal calf serum. The BT-20 cell line was grown in Eagle's Minimum Essential Medium (MEM) supplemented with 10% fetal calf serum. MCF7 cells were treated with 5-aza (2,5µM, SIGMA) for 72h and/or TSA (200mM, SIGMA) during 48h.

Transfection with pre-miRs

The individual precursors of miRNAs (pre-miRs) used in this study were purchased from Applied Biosystems. Cells were transfected with pre-miRs at 100 nM working concentration, using siPORT™ (Ambion) according to the manufacturer's protocol. Pre-miR negative control #1 (Ambion) was used as a scrambled control. Treatment proceeded for 72 h before RNA extraction and/or western blot analysis. It proceeded for 24 h before cell-based assays.

RNA purification and real-time quantitative PCR

Extraction of total RNA was carried out with the TriPure reagent (Roche) according to the manufacturer's instructions. DNase treatment was performed with a DNA-free DNase kit (Ambion) according to the manufacturer's protocol.

Quantitative PCRs were performed with SYBR Green dye (Eurogentec) on a LightCycler 480 (Roche). Briefly, cDNA was reverse transcribed from 1 µg RNA with random hexamers (Amersham/Pharmacia Biotech) and Superscript II reverse transcriptase (Life Technologies, Inc.). Real-time PCRs were performed to measure gene expression levels under different conditions. The primer sequences for the *KDM5B* and *KDM5C* amplifications were as follows: forward KDM5B, 5′-ACGTCGAATGGGTTGTCC-3′; reverse KDM5B, 5′-TCTTGGGCTTTTCCTTCTCA-3′; forward KDM5C, 5′-CAGATGAACAACCTGCCTTG-3′ ; reverse KDM5C, 5′-CCAGAACACCCTTGACATCC-3′. GAPDH was amplified as an internal control.

For microRNA quantitative PCRs, total RNA (10 ng) was reverse transcribed with the TaqMan MicroRNA Reverse Transcription Kit (Applied Biosystem) and miRNA-specific primers. For miRNA quantitation, the 7500 Fast Real-Time System (Applied Biosystem) was used in conjunction with gene-specific TaqMan assay kits for miR-137, miR-138, miR-329, and RNU6B. RNU6B was used as an endogenous control to normalize the expression of target microRNAs.

Cell extracts and western blot analyses

Whole-cell extracts were prepared with IPH lysis buffer (50 mM Tris-HCl pH 8, 150 mM NaCl, 5mM EDTA, 0.5% NP40). Nuclear extracts were prepared as follow : cells were first lysed in buffer A (10 mM HEPES pH 7.9, 10 mM Kcl, 0.1 mM EDTA, 1 mM DTT, protease inhibitors) and then centrifuged at 10,000 g for 5 min. Buffer B (20 mM HEPES pH7.9, 0.4 M NaCl, 1 mM EDTA, 10% glycerol, 1 mM DTT, protease inhibitors) was then added to the nuclear pellet fraction, then the mixture was shaken vigorously for 2 h and centrifuged at 12,000 g for 10 min. The supernatant (nuclear fraction) was stored at –80°C until used. All procedures were performed at 4°C.

Standard procedures were used for western blotting. The primary antibodies used in these experiments were against the following: KDM5B (Abnova, pAb-053-050), KDM5C (Abcam, ab34718), TBP (Abcam, ab818) and actin (Abcam, ab8226). Anti-TBP and anti-actin were used as loading control antibodies.

miR reporter luciferase assay

Complementary oligonucleotides containing the miR-137 target site of the KDM5B UTR (a 25-bp sequence from the KDM5B 3'UTR) were synthesized by Sigma. Oligonucleotides were annealed and ligated into the pMIR-REPORT luciferase reporter vector (Applied Biosystems). pMIR-REPORT Beta-Gal (Applied Biosystems) was used as a control to monitor transfection efficiency. Consructs were used to co-transfect MCF7 cells in a 24-well plate using siPORT. Briefly, cells were transfected with 100 nM miRNA precursor, 0.6 µg pMIR-3'UTR clone, and 0.4 µg pMIR-REPORT Beta-Gal for 48 h. The Dual-Light System Chemiluminescent Reporter Gene Assay was used according to the manufacturer's protocol to quantify luciferase and beta-galactosidase activity (Applied Biosystems).

The following oligonucleotides were used for cloning:

KDM5B_miR-137_F:

AATGCACTAGTCTAGGTTTATTTATCTGAGCAATAAGCTCAGCAAGCTTAATGC

KDM5B_miR-137_R:

GCATTAAGCTTGCTGAGCTTATTGCTCAGATAAATAAACCTAGACTAGTGCATT

Bisulfite pyrosequencing

750 ng genomic DNA was subjected to bisulfite conversion performed with the Epitect® Bisulfite Kit (Qiagen) according to the manufacturer's protocol. The converted DNA was generally eluted with 26 µl elution buffer, and 8 µl of the eluted DNA was used as template in subsequent PCRs. PCR and sequencing primers for bisulfite pyrosequencing were deduced with the PyroMark® Assay Design 2.0

software (Qiagen). Primers were obtained from Sigma. The following PCR and sequencing primers were used:

miR-137 Fwd: AGGGAAATAGAGTTATGGATTTATGGT ;

miR-137 Rev: [Btn]CACCCAAAAAAATCAAAAAACCAAACTAC and miR-137 sequencing primer: GGGTTTAGAGAGTAGTAAG.

PCRs were performed with the HotStarTaq PCR kit (Qiagen) according to the manufacturer's recommendations. Sample preparation and pyrosequencing reactions were performed with the Pyromark™ Q24 system (Qiagen).

Cell Proliferation and Migration assays

To evaluate breast cancer cell proliferation, MCF7 cells transfected with miRNA precursors were seeded 24 h post-transfection into the xCELLigence E-plate 16 (Roche) (8000 cells/well) according to the manufacturer's instructions. In this system, the electrical impedance is used to derive a cell index which, when continually monitored, gives a real-time representation of the growth characteristics of the cells. Measurements were automatically collected by the RTCA DP analyser every 30 min for up to 3 days. Four replicate measurements per condition were obtained. The data were analyzed with the provided RTCA software.

To examine breast cancer cell migration, MDA-MB-231 cells transfected with miRNA precursors were seeded 24 h post-transfection into the xCELLigence CIM-plate 16 (Roche). Briefly, a 165-µl volume of fresh medium containing 10% FBS (chemoattractant) or with serum-free medium (control) was added to the lower chambers of the CIM-plate 16. The upper chambers were filled with serum-free medium (30 µl/well) and the plate was incubated at 37°C in 5% CO2 for 1 h. Cells (40000 cells/well) were then added to each well of the upper chamber. After 30 min, the CIM plate was assembled onto the RTCA DP analyser and cell migration was assessed at 30-min intervals for 4 h at 37°C in 5% CO2. Upon migration, cells adhere to the surface of the filter electrode and increase the

impedance (Fig. S5). Four replicate measurements per condition were obtained. The data were analyzed with the provided RTCA software. When analyzing serum-induced migration data, it is important to choose a migration time well below the doubling time of the cells in order to capture signals derived from cell migration only, rather than both cell migration and proliferation (recommended by the xCELLigence supplier). We therefore focused on the first 4 hours of the migration kinetics to calculate the rate of MDA-MB-231 migration.

Statistics

Student tests were used to perform statisitcal analysis. * is indicated if $p<0,05$.

Acknowledgements

We thank Michael Volkmar and ‘Matladi N. Ndlovu for their helpful advices.

Funding

H.D. was supported by the Belgian Fonds National de la Recherche Scientifique and the Brussels Region, S.D. by the Télévie and the Innoviris/Brubreast grant and R.D. by the Interuniversity Attraction Poles [IUAP P6/28] and the Télévie. B.D is a Research Fellow from the Fonds National de la Recherche Scientifique. F.F. is a Professor of the “Université Libre de Bruxelles”. This work was funded by grants from the Fonds National de la Recherche Scientifique and Télévie, the “Plan National Cancer”, the IAP P7/03, by the Brussels Region, by the Belgian Fndation against Cancer and by the «Action de Recherche Concertée». Funding for open access charge:Belgian ARC.

Conflicts of interest

The authors declare that they have no conflicts of interest.

References

1 G. Felsenfeld and M. Groudine, *Nature*, 2003, **421**, 448–453.

2 P. Chi, C. D. Allis and G. G. Wang, *Nat Rev Cancer*, 2010, **10**, 457–469.

3 R. A. Varier and H. T. M. Timmers, *Biochim Biophys Acta*, 2011, **1815**, 75–89.

4 K. Collett, G. E. Eide, J. Arnes, I. M. Stefansson, J. Eide, A. Braaten, T. Aas, A. P. Otte and L. A. Akslen, *Clin Cancer Res*, 2006, **12**, 1168–1174.

5 C. G. Kleer, Q. Cao, S. Varambally, R. Shen, I. Ota, S. A. Tomlins, D. Ghosh, R. G. Sewalt, A. P. Otte, D. F. Hayes, M. S. Sabel, D. Livant, S. J. Weiss, M. A. Rubin and A. M. Chinnaiyan, *Proc Natl Acad Sci U S A*, 2003, **100**, 11606–11611.

6 T. Suzuki, M. Terashima, S. Tange and A. Ishimura, *Cancer Sci.*, 2013, **104**, 795–800.

7 S. Lim, E. Metzger, R. Schule, J. Kirfel and R. Buettner, *Int J Cancer*, **127**, 1991–1998.

8 J. H. Schulte, S. Lim, A. Schramm, N. Friedrichs, J. Koster, R. Versteeg, I. Ora, K. Pajtler, L. Klein-Hitpass, S. Kuhfittig-Kulle, E. Metzger, R. Schule, A. Eggert, R. Buettner and J. Kirfel, *Cancer Res*, 2009, **69**, 2065–2071.

9 S. Amente, G. Milazzo, M. C. Sorrentino, S. Ambrosio, G. Di Palo, L. Lania, G. Perini and B. Majello, *Oncotarget*, 2015, **6**, 14572–14583.

10 R. J. Klose, E. M. Kallin and Y. Zhang, *Nat Rev Genet*, 2006, **7**, 715–727.

11 L. J. van Zutven, E. Onen, S. C. Velthuizen, E. van Drunen, A. R. von Bergh, M. M. van den Heuvel-Eibrink, A. Veronese, C. Mecucci, M. Negrini, G. E. de Greef and H. B. Beverloo, *Genes Chromosom. Cancer*, 2006, **45**, 437–446.

12 G. G. Wang, J. Song, Z. Wang, H. L. Dormann, F. Casadio, H. Li, J. L. Luo, D. J. Patel and C. D. Allis, *Nature*, 2009, **459**, 847–851.

13 J. Zeng, Z. Ge, L. Wang, Q. Li, N. Wang, M. Bjorkholm, J. Jia and D. Xu, *Gastroenterology*, **138**, 981–992.

14 W. Lin, J. Cao, J. Liu, M. L. Beshiri, Y. Fujiwara, J. Francis, A. D. Cherniack, C. Geisen, L. P. Blair, M. R. Zou, X. Shen, D. Kawamori, Z. Liu, C. Grisanzio, H. Watanabe, Y. A. Minamishima, Q. Zhang, R. N. Kulkarni, S. Signoretti, S. J. Rodig, R. T. Bronson, S. H. Orkin, D. P. Tuck, E. V Benevolenskaya, M. Meyerson, W. G. Kaelin Jr. and Q. Yan, *Proc Natl Acad Sci U S A*, **108**, 13379–13386.

15 A. Barrett, B. Madsen, J. Copier, P. J. Lu, L. Cooper, A. G. Scibetta, J. Burchell and J. Taylor-Papadimitriou, *Int J Cancer*, 2002, **101**, 581–588.

16 S. Hayami, M. Yoshimatsu, A. Veerakumarasivam, M. Unoki, Y. Iwai, T. Tsunoda, H. I. Field, J. D. Kelly, D. E. Neal, H. Yamaue, B. A. Ponder, Y. Nakamura and R. Hamamoto, *Mol Cancer*, **9**, 59.

17 P. J. Lu, K. Sundquist, D. Baeckstrom, R. Poulsom, A. Hanby, S. Meier-Ewert, T. Jones, M. Mitchell, P. Pitha-Rowe, P. Freemont and J. Taylor-Papadimitriou, *J Biol Chem*, 1999, **274**, 15633–15645.

18 Z. Wang, F. Tang, G. Qi, S. Yuan, G. Zhang, B. Tang and S. He, *Am. J. Cancer Res.*, 2015, **5**, 87–100.

19 K. Yamane, K. Tateishi, R. J. Klose, J. Fang, L. A. Fabrizio, H. Erdjument-Bromage, J. Taylor-Papadimitriou, P. Tempst and Y. Zhang, *Mol Cell*, 2007, **25**, 801–812.

20 W. Filipowicz, S. N. Bhattacharyya and N. Sonenberg, *Nat Rev Genet*, 2008, **9**, 102–114.

21 E. Huntzinger and E. Izaurralde, *Nat Rev Genet*, **12**, 99–110.

22 A. Ventura and T. Jacks, *Cell*, 2009, **136**, 586–591.

23 M. S. Nicoloso, R. Spizzo, M. Shimizu, S. Rossi and G. A. Calin, *Nat Rev Cancer*, 2009, **9**, 293–302.

24 Q. Huang, K. Gumireddy, M. Schrier, C. le Sage, R. Nagel, S. Nair, D. A. Egan, A. Li, G. Huang, A. J. Klein-Szanto, P. A. Gimotty, D. Katsaros, G. Coukos, L. Zhang, E. Pure and R. Agami, *Nat Cell Biol*, 2008, **10**, 202–210.

25 L. Ma, J. Teruya-Feldstein and R. A. Weinberg, *Nature*, 2007, **449**, 682–688.

26 J. Lu, G. Getz, E. A. Miska, E. Alvarez-Saavedra, J. Lamb, D. Peck, A. Sweet-Cordero, B. L. Ebert, R. H. Mak, A. A. Ferrando, J. R. Downing, T. Jacks, H. R. Horvitz and T. R. Golub, *Nature*, 2005, **435**, 834–838.

27 J. Le Quesne and C. Caldas, *Mol Oncol*, **4**, 230–241.

28 E. O'Day and A. Lal, *Breast Cancer Res*, **12**, 201.

29 K. Kozaki, I. Imoto, S. Mogi, K. Omura and J. Inazawa, *Cancer Res*, 2008, **68**, 2094–2105.

30 F. Balaguer, A. Link, J. J. Lozano, M. Cuatrecasas, T. Nagasaka, C. R. Boland and A. Goel, *Cancer Res*, **70**, 6609–6618.

31 E. Bandres, X. Agirre, N. Bitarte, N. Ramirez, R. Zarate, J. Roman-Gomez, F. Prosper and J. Garcia-Foncillas, *Int J Cancer*, 2009, **125**, 2737–2743.

32 J. Ferlay, D. M. Parkin and E. Steliarova-Foucher, *Eur J Cancer*, **46**, 765–781.

33 J. Ferlay, H. R. Shin, F. Bray, D. Forman, C. Mathers and D. M. Parkin, *Int J Cancer*, **127**, 2893–2917.

34 B. T. Bilynskyj, *Exp Oncol*, **32**, 190–194.

35 P. A. Jones and S. B. Baylin, *Cell*, 2007, **128**, 683–692.

36 T. Ando, T. Yoshida, S. Enomoto, K. Asada, M. Tatematsu, M. Ichinose, T. Sugiyama and T. Ushijima, *Int J Cancer*, 2009, **124**, 2367–2374.

37 R. Steponaitiene, J. Kupcinskas, C. Langner, F. Balaguer, L. Venclauskas, H. Pauzas, A. Tamelis, J. Skieceviciene, L. Kupcinskas, P. Malfertheiner and A. Link, *Mol. Carcinog.*, 2015.

38 N. Kang, S. Y. Choi, Y. K. Kim, I. R. Yoo, D. H. Han, D. S. Lee, Y. S. Kim, S. H. Hong, J. H. Kang, K. Y. Lee, J. K. Park, S. W. Sung, M. S. Park, H. W. Yim, S. J. Kim and J. Y. Park, *Lung Cancer*, 2015.

39 P. Mestdagh, A. K. Bostrom, F. Impens, E. Fredlund, G. Van Peer, P. De Antonellis, K. von Stedingk, B. Ghesquiere, S. Schulte, M. Dews, A. Thomas-Tikhonenko, J. H. Schulte, M. Zollo, A. Schramm, K. Gevaert, H. Axelson, F. Speleman and J. Vandesompele, *Mol Cell*, **40**, 762–773.

40 G. Martin-Manso, M. J. Calzada, Y. Chuman, J. M. Sipes, C. P. Xavier, V. Wolf, S. A. Kuznetsova, J. S. Rubin and D. D. Roberts, *Arch Biochem Biophys*, **509**, 147–156.

41 C. M. Croce, *Nat Rev Genet*, 2009, **10**, 704–714.

42 L. T. Bemis, R. Chen, C. M. Amato, E. H. Classen, S. E. Robinson, D. G. Coffey, P. F. Erickson, Y. G. Shellman and W. A. Robinson, *Cancer Res*, 2008, **68**, 1362–1368.

43 M. Liu, N. Lang, M. Qiu, F. Xu, Q. Li, Q. Tang, J. Chen, X. Chen, S. Zhang, Z. Liu, J. Zhou, Y. Zhu, Y. Deng, Y. Zheng and F. Bi, *Int J Cancer*, **128**, 1269–1279.

44 C. Tarantino, G. Paolella, L. Cozzuto, G. Minopoli, L. Pastore, S. Parisi and T. Russo, *FASEB J*, **24**, 3255–3263.

45 G. Sun, P. Ye, K. Murai, M. F. Lang, S. Li, H. Zhang, W. Li, C. Fu, J. Yin, A. Wang, X. Ma and Y. Shi, *Nat Commun*, **2**, 529.

46 A. Derfoul, A. H. Juan, M. J. Difilippantonio, N. Palanisamy, T. Ried and V. Sartorelli, *Carcinogenesis*, **32**, 1607–1614.

47 D. P. Bartel, *Cell*, 2009, **136**, 215–233.

48 C. A. Andorfer, B. M. Necela, E. A. Thompson and E. A. Perez, *Trends Mol Med*, **17**, 313–319.

49 S. Iwase, F. Lan, P. Bayliss, L. de la Torre-Ubieta, M. Huarte, H. H. Qi, J. R. Whetstine, A. Bonni, T. M. Roberts and Y. Shi, *Cell*, 2007, **128**, 1077–88.

50 S. Catchpole, B. Spencer-Dene, D. Hall, S. Santangelo, I. Rosewell, M. Guenatri, R. Beatson, A. G. Scibetta, J. M. Burchell and J. Taylor-Papadimitriou, *Int. J. Oncol.*, 2011, **38**, 1267–77.

51 M. R. Zou, J. Cao, Z. Liu, S. J. Huh, K. Polyak and Q. Yan, *J. Biol. Chem.*, 2014, **289**, 17620–33.

52 M. Fabbri, R. Garzon, A. Cimmino, Z. Liu, N. Zanesi, E. Callegari, S. Liu, H. Alder, S. Costinean, C. Fernandez-Cymering, S. Volinia, G. Guler, C. D. Morrison, K. K. Chan, G. Marcucci, G. A. Calin, K. Huebner and C. M. Croce, *Proc Natl Acad Sci U S A*, 2007, **104**, 15805–15810.

53 R. Garzon, S. Liu, M. Fabbri, Z. Liu, C. E. Heaphy, E. Callegari, S. Schwind, J. Pang, J. Yu, N. Muthusamy, V. Havelange, S. Volinia, W. Blum, L. J. Rush, D. Perrotti, M. Andreeff, C. D. Bloomfield, J. C. Byrd, K. Chan, L. C. Wu, C. M. Croce and G. Marcucci, *Blood*, 2009, **113**, 6411–6418.

54 S. Varambally, Q. Cao, R. S. Mani, S. Shankar, X. Wang, B. Ateeq, B. Laxman, X. Cao, X. Jing, K. Ramnarayanan, J. C. Brenner, J. Yu, J. H. Kim, B. Han, P. Tan, C. Kumar-Sinha, R. J. Lonigro, N. Palanisamy, C. A. Maher and A. M. Chinnaiyan, *Science (80-.).*, 2008, **322**, 1695–1699.

55 E. J. Noonan, R. F. Place, D. Pookot, S. Basak, J. M. Whitson, H. Hirata, C. Giardina and R. Dahiya, *Oncogene*, 2009, **28**, 1714–1724.

Figures Legends

Fig 1. MiR-137 is downregulated in breast cancer. (A) miR-137 expression was analysed by TaqMan RT-qPCR in non-tumorigenic human mammary epithelial cell line (MCF10A) and in five breast cancer cell lines (MCF7, MDA-MB-361, BT20, SKBR3, and ZR-75-1). Results are normalized with respect to the endogenous control RNU6B presented in the bottom panel (copy number) for direct comparaison. (*=p<0,05) (n=3). **(B** Upper part: Map of the miR-137 promoter, with the position of the CpG island and the region used for methylation analysis indicated. The USCS genome browser was used to identify the upstream CpG island. Lollipops represent all the CG dinucleotides. Lower part: Methylation levels of the miR-137 promoter in the MCF12A, MCF10A, MCF7, MDA-MB-361, BT20, and ZR-75-1 breast cell lines. A representative experiment is shown.

Fig 2. MiR-137 regulates breast cancer cell proliferation and migration. (A) Cell index (mean ± standard deviation) as a measure of MCF7 cell proliferation. Measurements were automatically collected by the RTCA DP analyser every 30 min for up to 3 days (n=4). Black: MCF-7 cells transfected with control pre-miR (ctrl pre-miR); Red: MCF7 cells transfected with precursors of miR-137 (pre-miR-137). **(B)** Results of the cell proliferation assays represented as slopes (changes in cell index/hour) (n=3) (*= p<0,05). **(C)** Migration kinetics of MDA-MB-231 cells assessed by continuous monitoring of live cell migration for approximately 24 hours. Black: MDA-MB-231 cells transfected with control pre-miR (ctrl pre-miR + FBS), 10% FBS in lower chamber (LC), n=4 ; Red: MDA-MB-231 cells transfected with miR-137 precursors (pre-miR-137 + FBS), 10% FBS in LC, n=4. Negative controls: grey: MDA-MB-231 cells transfected with control pre-miR (ctrl pre-miR - FBS), serum-free medium in LC, n=2; Yellow: MDA-MB-231 cells transfected with miR-137 precursors (pre-miR-137 - FBS), SFM in LC, n=2. **(D)** Results of the cell migration assays represented as slopes (changes in cell index/hour) (n=3) (*= p<0,05).

Fig 3. KDM5B is a direct target of miR-137 in breast cancer cells. (A) Immunoblot analysis of KDM5B protein levels in MCF10A, BT20, MCF7, MDA-MB-231, MDA-MB-361, SKBR3, and ZR-75-1 cell lines. Vertical line indicates juxtaposition of lanes non-adjacent within the same blot, exposed for the same time. **(B)** Following transfection of MCF7 cells with miR-137 precursors (pre-miR-137) or with a scrambled pre-miR used as a negative control (ctrl pre-miR), KDM5B mRNA levels were

analysed by real-time qPCR and standardized with respect to the endogenous control GAPDH. Relative expression levels were determined for control-pre-miR- and pre-miR-137-transfected cells. (n=3) (*= p<0,05) **(C)** KDM5B protein levels in MCF7 cells were assessed by western blotting following transfection of MCF7 cells with control pre-miR or pre-miR-137. TBP was used as a loading control. **(D)** a 25-bp sequence from the KDM5B 3'UTR was cloned into the 3'UTR of a luciferase reporter vector (upper part). MCF7 cells were transfected with ctrl pre-miR or pre-miR-137 together with the pMIR-3'UTR construct and pMIR-REPORT Beta-Gal. Luciferase activity was assayed 48 h post-transfection and normalized with respect to beta-galacosidase activity. Relative luciferase activity was determined on control-pre-miR- and pre-miR-137-transfected samples (n=3) (*= p<0,05).

Fig 4. MiR-138 regulates the histone demethylase KDM5C in breast cancer cells. (A) Immunoblot analysis of KDM5C protein levels in the MCF10A, BT20, MCF7, MDA-MB-231, MDA-MB-361, SKBR3, and ZR-75-1 cell lines. **(B)** miR-138 levels were analysed by TaqMan RT-qPCR in the non-tumorigenic human mammary epithelial cell line (MCF10A) and in several breast cancer cell lines (MCF7, MDA-MB-361, BT20, SKBR3, and ZR-75-1). Results are normalized with respect to the endogenous control RNU6B shown in the bottom part (copy number) (*=p<0,05) (n=3). The bottom panel shown the level of RNU6B expression (copy number) for direct comparison. **(C)** Following transfection of MCF7 cells with miRNA precursors (pre-miR-138) or nonspecific control (ctrl pre-miR), KDM5C mRNA levels were analysed by qPCR and normalized with respect to the endogenous control GAPDH. (n=3) (*= p<0,05) **(D)** MCF7 cells were transfected with pre-miR-138, or the negative control and then western blot analysis was performed to detect KDM5C. **(E)** A 25-bp sequence from the KDM5C 3'UTR was cloned into the 3'UTR of a luciferase reporter vector (upper part). MCF7 cells were transfected with ctrl pre-miR or pre-miR-138 together with the pMIR-3'UTR construct and pMIR-REPORT Beta-Gal. Luciferase activity was assayed 48 h post-transfection and normalized with respect to beta-galacosidase activity. Relative luciferase activity was determined on control-pre-miR- and pre-miR-138-transfected samples (n=3) (*= p<0,05).

Fig 5. MiR-138 regulates breast cancer cell proliferation. (A) Cell index (mean ± standard deviation) as a measure of the growth of MCF7 cells. Measurements were automatically collected by the RTCA DP analyzer every 30 min for up to 3 days (n=4). Black: MCF-7 cells transfected with control pre-miR; Green: MCF7 cells transfected with precursors of miR-138 (pre-miR-138). **(B)** Results

of the cell proliferation assays are represented as slopes (changes in cell index/hour) (n=3) (*= p<0,05).

Electronic Supplementary Information

Electronic Supplementary Information for this article can be accessed on the publisher's website.

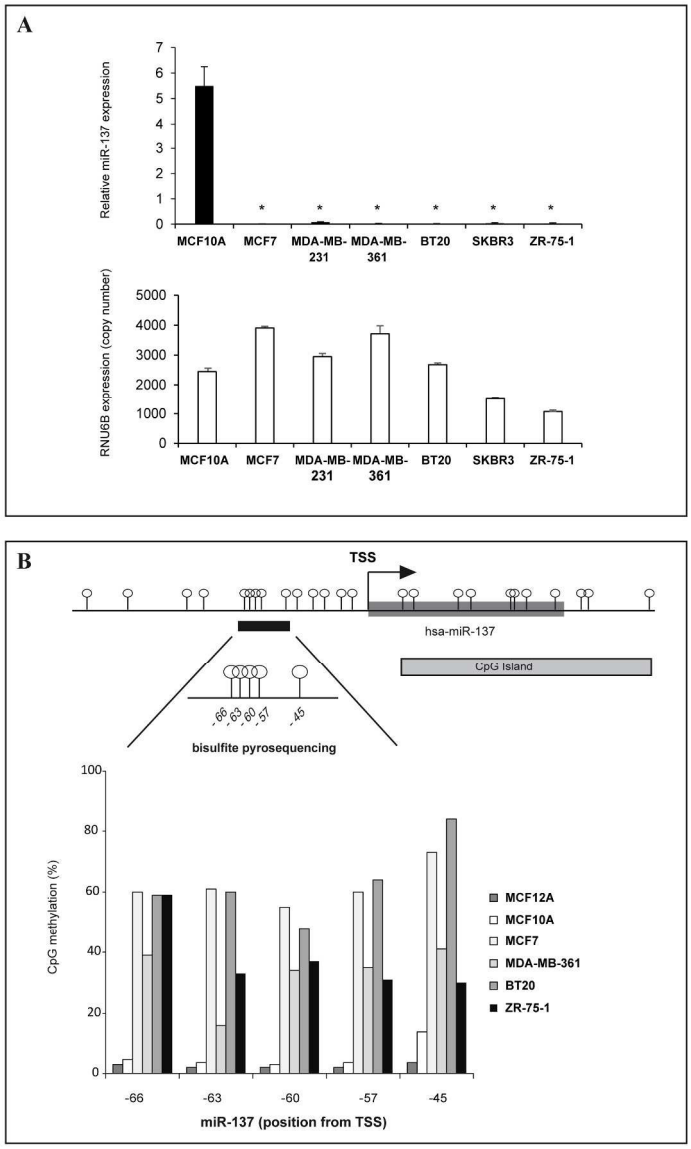

Figure 1, Denis *et al.*

170x274mm (300 x 300 DPI)

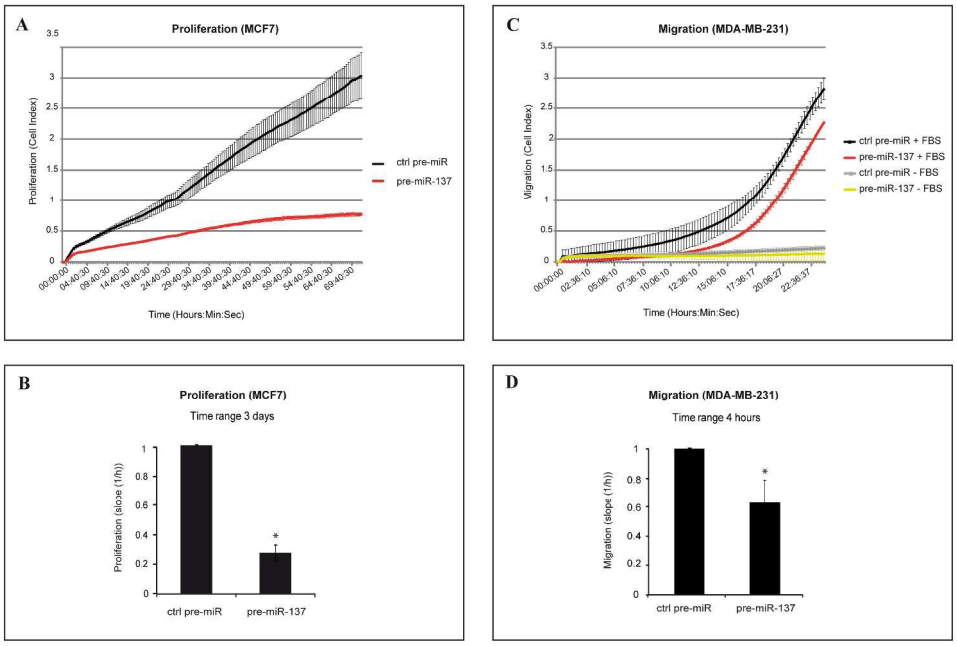

Figure 2, Denis *et al.*

284x199mm (300 x 300 DPI)

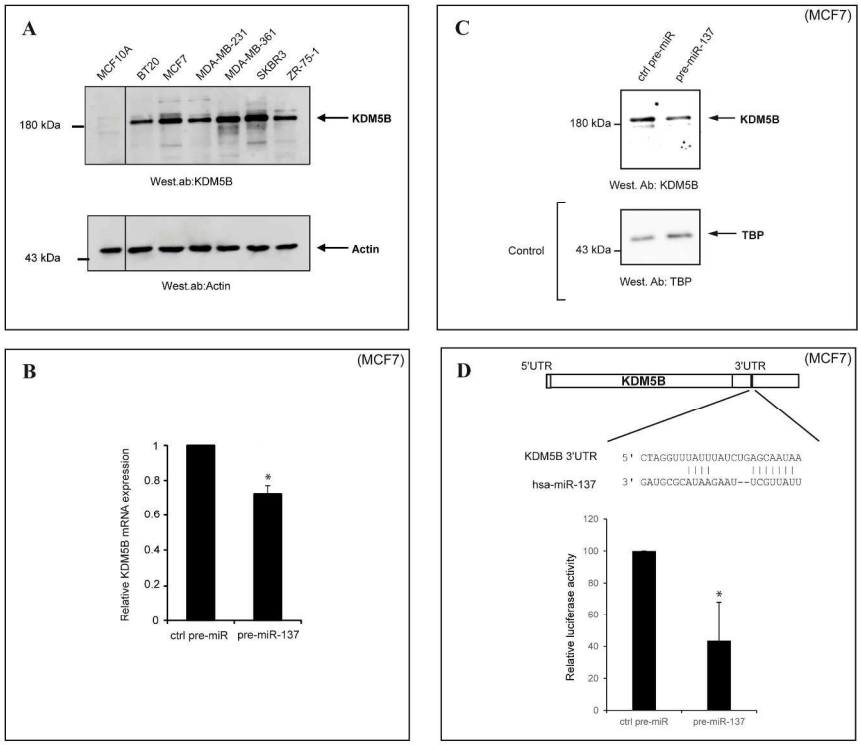

Figure 3, Denis *et al.*

253x208mm (300 x 300 DPI)

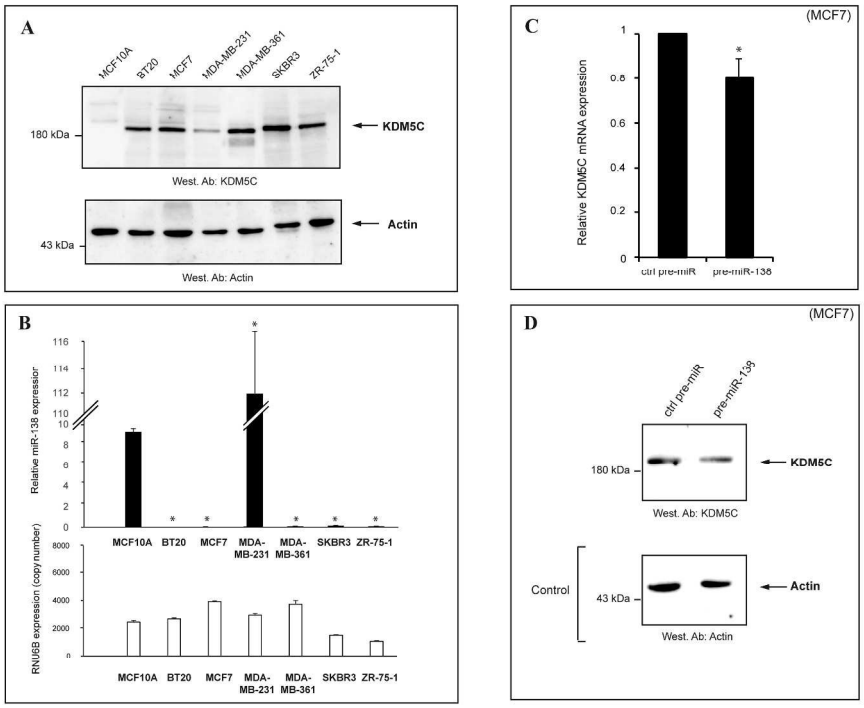

Figure 4A-D, Denis *et al.*

267x206mm (300 x 300 DPI)

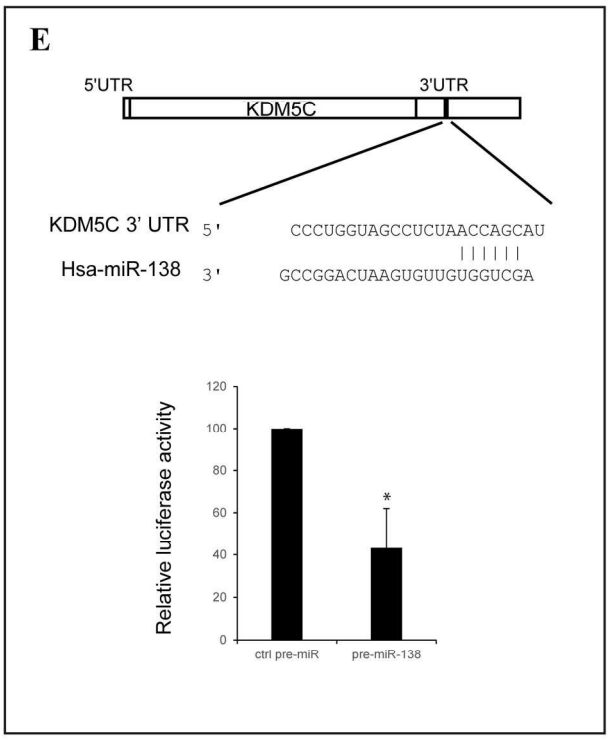

Figure 4E, Denis *et al.*

159x194mm (300 x 300 DPI)

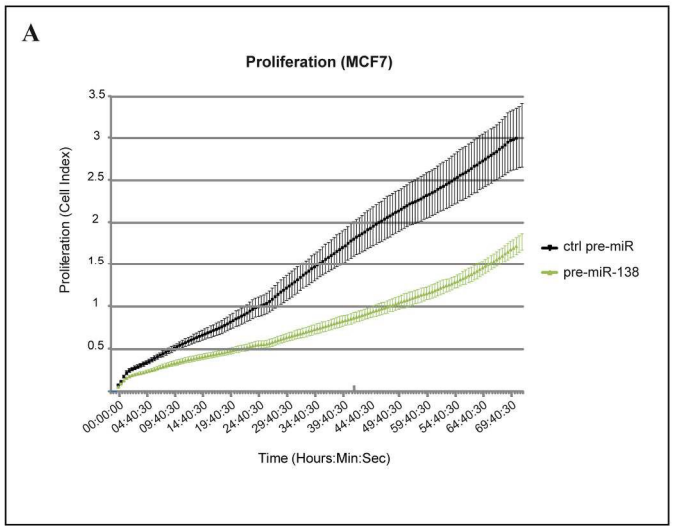

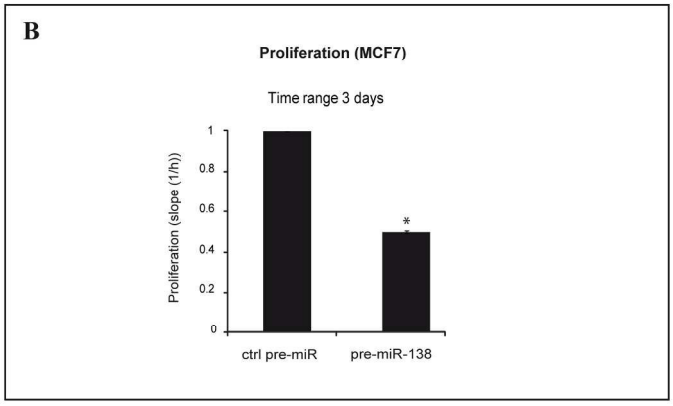

Figure 5, Denis *et al.*

163x247mm (300 x 300 DPI)